Monitoring the Channel Formation in Organic Field-Effect Transistors via Photoinduced Charge Transfer

By *Thokchom Birendra Singh,* Robert Koeppe, Niyazi Serdar Sariciftci, Mauro Morana,* and *Christoph J. Brabec*

Conducting channel formation in organic field-effect transistors (OFETs) is considered to happen in the organic semiconductor layer very close to the interface with the gate dielectric. In the gradual channel approximation, the local density of accumulated charge carriers varies as a result of applied gate bias, with the majority of the charge carriers being localized in the first few semiconductor monolayers close to the dielectric interface. In this report, a new concept is employed which enables the accumulation of charge carriers in the channel by photoinduced charge transfer. An OFET employing C_{60} as a semiconductor and divinyltetramethyldisiloxane-bis(benzocyclobutene) as the gate dielectric is modified by a very thin noncontinuous layer of zinc-phthalocyanine (ZnPc) at the semiconductor/dielectric interface. With this device geometry, it is possible to excite the phthalocyanine selectively and photogenerate charges directly at the semiconductor/dielectric interface via photoinduced electron transfer from ZnPc onto C_{60}. Thus the formation of a gate induced and a photoinduced channel in the same device can be correlated.

1. Introduction

Ultrafast photoinduced charge transfer (PICT) at the interface of thin films of conjugated polymers with fullerenes or conjugated polymers with semiconductor nanoparticles is a well-studied phenomenon, and one which is essential for organic or hybrid organic/inorganic solar cells,[1] photodiodes,[2] phototransistors,[3] and flexible image sensors.[4] All of these devices usually employ a heterojunction between an electron donor and an electron acceptor at which charge carriers are generated under illumination and afterwards extracted. The number of photogenerated charges that can be collected from the device is dependent on the photoexcitation rate, the charge transfer rate, the charge carrier extraction time, and the recombination rate of the photogenerated charge carriers. The excitation rate is given by the product of the absorption coefficient, α (dependent on photon energy), and the photon flux density, ϕ per unit area per unit time. If the energy levels of donor and acceptor moieties are well tuned, the charge transfer rate can be much higher than the recombination rate, so nearly every absorbed photon is creating a pair of free charge carriers. The time for the extraction of the charge carriers can be measured by time-resolved photocurrent studies[5] and is usually the main limiting factor for the internal quantum efficiency (IQE, the ratio between collected charges and photons absorbed in the active layer of the device). The external quantum efficiency (EQE, also the incident photon to collected electron efficiency IPCE)[6] is additionally dependent on the absorption properties of the device and can be directly measured.

The aforementioned dependencies are well studied in multilayer thin film diode structures. Here we report on measurements of the photogeneration processes in a thin film transistor by studying the interface between donor and acceptor molecules at its conducting channel. Charge accumulation and transport in organic field-effect transistors (OFETs) is well known to occur within the first few semiconductor monolayers at the interface of the gate dielectric.[7–10] In the present experiment, we build OFET devices that allow the measurement of both processes of field-induced and photoinduced charge accumulation independently or simultaneously. The device consists of an active semiconducting acceptor layer and islands of donor molecules in the conducting channel of the OFET. ZnPc was chosen as donor and C_{60} both as acceptor and active transport layer. An additional advantage of this material combination is that upon illumination with monochromatic light at 780 nm, only the ZnPc is excited, leading to a photoinduced charge generation occurirng at the C_{60}/ZnPc interface and very close to the semiconductor/dielectric (BCB) interface. The OFET can thus be gated in two ways: either by applying a gate voltage, V_{gate} (electrical gating) or by illuminating the device (photogating). The experiments allow us to visualize the conducting channel formation in the active semiconductor layer at the interface of the gate dielectric upon

[*] Dr. Th. B. Singh,[+] Dr. R. Koeppe, Prof. N. S. Sariciftci
Linz Institute of Organic Solar Cells (LIOS)
Institute of Physical Chemistry
Johannes Kepler University, Linz A 4040 (Austria)
E-mail: birendra.singh@csiro.au
Dr. M. Morana, Dr. C. J. Brabec
Konarka Technologies, Altenbergerstrasse 69
Linz A 4040 (Austria)

[+] Current address: Molecular and Health Technologies, CSIRO, Ian Wark Laboratory, Bayview Ave., Clayton, VIC 3168 (Australia)

DOI: 10.1002/adfm.200801438

applied V_{gate} in OFETs. Additionally, from the measurement of gate field-induced charges, V_{gate} equivalent photoinduced charges as a function of ϕ and hence the EQE as well as IQE of photocurrent generation can be derived.

Light response in OEFTs is of interest from both a fundamental science as well as from an application point of view.[11–32] From the application side, a distinct feature of the light sensing properties of OFETs is that the responsivity, R, which is defined as J_{ph}/P where, J_{ph} is the photocurrent density (total drain current, I_{drain} upon illumination minus the dark current per unit area) and P is the power density, can be tuned by orders of magnitude by an applied V_{gate}. From the fundamental point of view so far very little is known about the origin of the nature of charge transport under illumination and whether it is unipolar or ambipolar.[11] Ambipolar transport is sensitive to the interface between the organic semiconductor and the gate dielectric[33] as well as the nature of the traps.[34] Likewise, in the studies of photoresponse, an observation of high R[22] can be affected by electron trapping at the interface near the gate dielectric layer[17] and the electrode work function.[20] A photovoltaic effect[35] and high R[36,37] are reported on ambipolar transistors based on a bulk heterojunction concept. In the present studies, we have chosen a bilayer concept to study the conducting channel formation of OFETs with C_{60} as active semiconductor and islands of zinc pthalocyanine ZnPc in the interface between semiconductor and gate dielectric. Although one might expect adverse effects on charge transport by the additional ZnPc islands we have achieved even better transistor characteristics in addition to its functioning as a PICT layer.

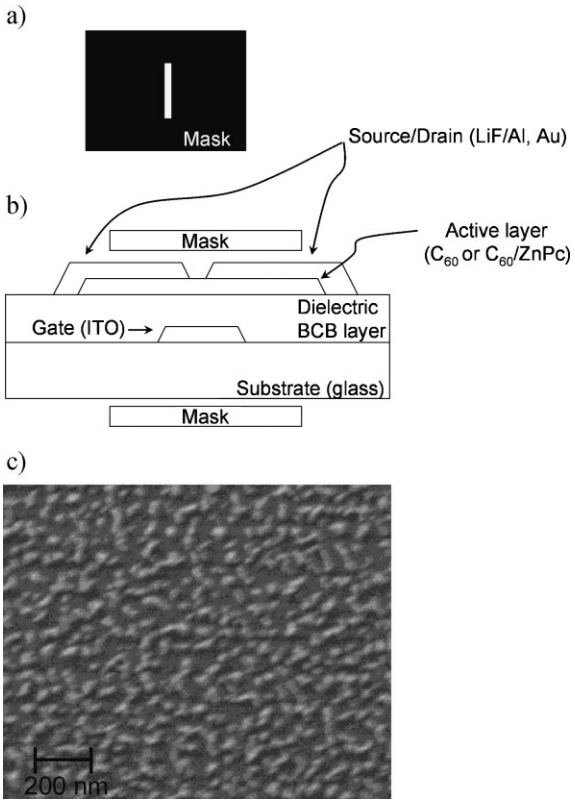

Figure 1. a) The scheme of the mask used to illuminate the transistor only in the channel area. b) Device scheme of the C_{60}-based OFET; two types of OFETs were fabricated: one with the active single layer C_{60}, and another one with bilayer which comprises 5 nm ZnPc layer inserted between BCB and active C_{60} layer. c) Surface electron micrograph of ZnPc islands grown on BCB dielectric.

2. Results and Discussion

2.1. Single Layer and Bilayer OFETs in Saturation Regime and Under Dark

A BCB layer was employed as an optically transparent dielectric. The two chosen semiconductors C_{60}[38] and ZnPc[39] as well as BCB[38,40] as dielectric have previously been studied. A scheme of the device is depicted in Figure 1. To avoid any unwanted contact effects, a shadow mask, as shown in Figure 1a, was used which allows illumination of only the channel area of the OFETs, as depicted in Figure 1b. From the studies of the surface nanomorphology on the completed devices, the BCB dielectric shows rather smooth films.[41] Scanning electron microscopy (SEM) reveals the formation of islands of ZnPc on the surface of BCB as shown in Figure 1c. It is well known that phthalocyanine usually grows in a Volmer-Weber mechanism, forming irregular grains around the nucleation sites with a percolated film appearing only after deposition of an equivalent film thickness greater than 10 nm.[42] The charge transfer between C_{60} and ZnPc is well studied[43] and the absorption spectra are shown in Figure 2. The absorption onset of C_{60} is at 720 nm[44] while ZnPc is still strongly absorbing also at higher wavelengths which allows us to photoexcite exclusively ZnPc with an excitation wavelength of 780 nm. On the other hand, both the films can be photoexcited simultaneously with illumination at 532 nm. First we compare the transistor characteristics in the dark for C_{60} single layer and

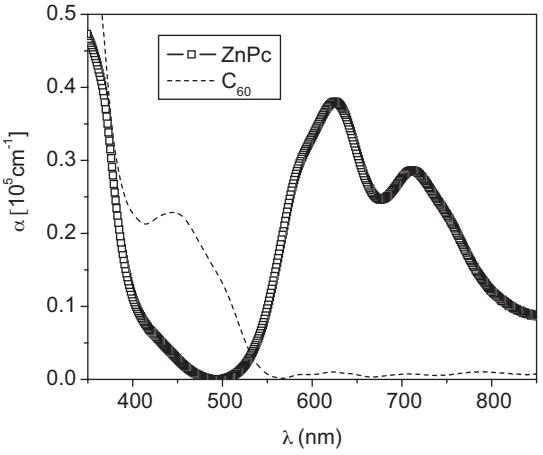

Figure 2. Absorption coefficient (α) for 300-nm C_{60} film grown on BCB dielectric and 5-nm ZnPc grown on BCB dielectric showing ZnPc absorbing wavelength greater than 850 nm.

bilayer OFETs. Single layer OFETs show on-currents in the order of 10^{-5} A and off-currents in the order of 10^{-9} A, this means an on/off ratio $>10^4$. Transistor characteristics of the bilayer devices show on/off ratios in the same order. The saturated

regime *mobilities*, μ_{FE} calculated using the standard transistor equations:

$$I_{drain} = \frac{\mu_{FE} C_{ins} W}{2L}\left[(V_{gate} - V_{th})V_{drain} - \frac{V_{drain}^2}{2}\right], \quad V_{drain} < V_{gate} \tag{1}$$

and

$$I_{drain} = \frac{\mu_{FE} C_{ins} W}{2L}\left[\frac{(V_{gate} - V_{th})^2}{2}\right], V_{drain} < V_{gate} \tag{2}$$

are 0.6 and 0.3 $cm^2 V^{-1} s^{-1}$ with threshold voltages, V_{th}, of 13 and 0 V for single layer and bilayer OFETs, respectively.

2.2. Single Layer and Bilayer OFETs in Saturation Regime and Upon Illumination

For the two devices we compare the photoresponse with 532 nm excitation as shown in Figure 3. The bilayer devices show a 15 times higher photoresponse in the depletion regime and 2 times higher *R* in the accumulation regime compared to the single layer OFETs, which mainly due to PICT.[43,44] The shadow mask used to illuminate only the OFET channel area is important to avoid many possible side effects such as diffusion length[26] and contact effects.[45] Having reported a high *R*, it is also noticed that previous reports[11,23] have illuminated the device without a mask.

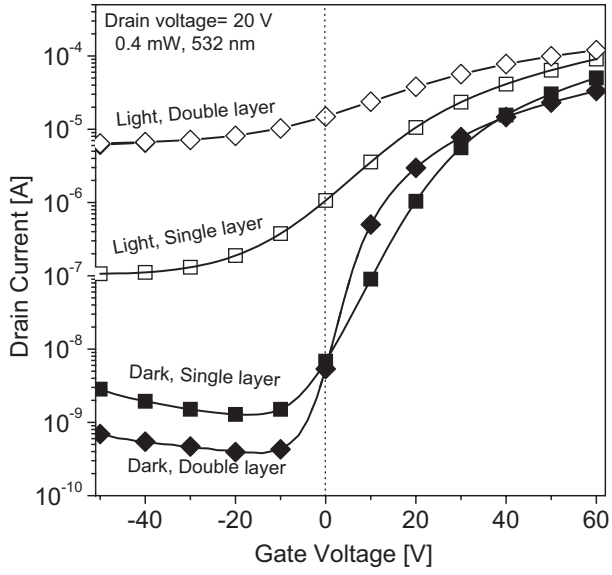

Figure 3. Comparison of transfer characteristics in the saturation regime ($V_D = 20$ V) of single layer and bilayer structured devices under dark and upon illumination (without mask) of 532 nm with an intensity of 0.4 mW. Note that OFET is operating in the saturation regime with applied drain voltage of 20 V. Insertion of ZnPc layer/islands inhibits photoinduced electron transfer at the interface of ZnPc and C_{60} giving rise to enhanced drain current. The bilayer devices show a 15 times higher photoresponse in the depletion regime and 2 times higher *R* in the accumulation regime compared to the single layer OFETs mainly due to PICT [43, 44].

Figure 4a shows the comparison of the OFET transfer characteristics upon illumination in the saturation regime of bilayer devices with and without mask. The light response is comparable for the both of the devices with and without mask in its accumulation regime. However, the devices without mask show a large photoresponse in the depletion regime of the OFET.

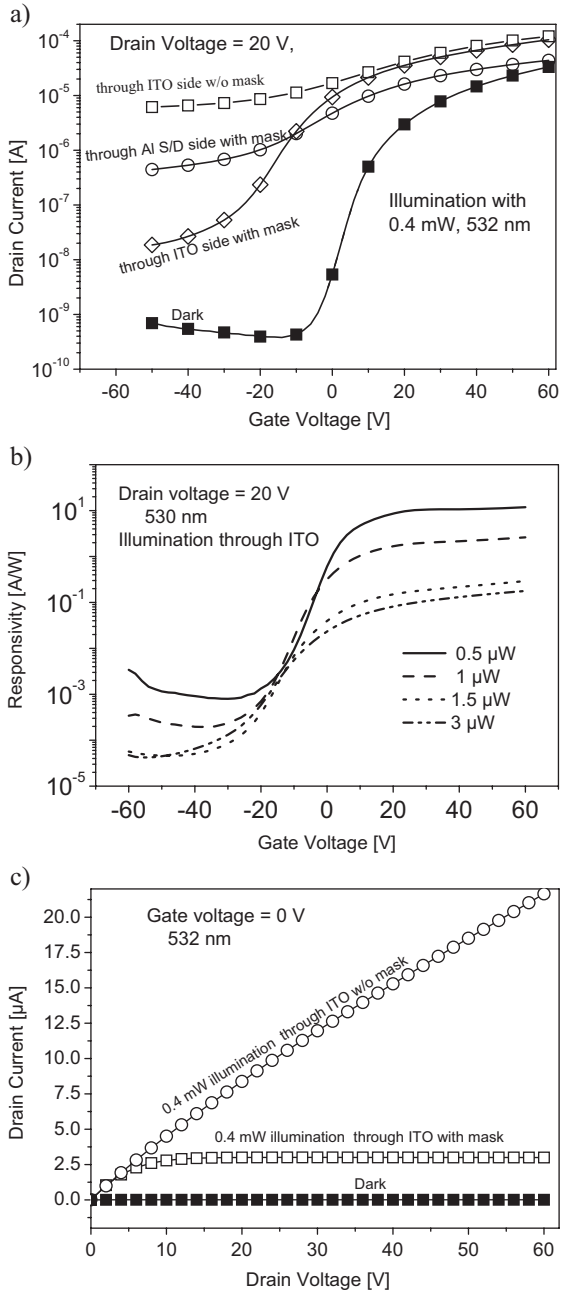

Figure 4. a) Comparison of transfer characteristics in the saturation regime ($V_D = 20$ V) of bilayer devices with and without mask upon illumination of 532 nm light, intensity of 0.4 mW. b) Plot of responsivity versus gate bias voltage for different intensity for the masked device. c) Comparison of the output characteristics for the devices with and without mask under dark and upon illumination of 532 nm, 0.4 mW light.

This observation can be attributed to many effects such as reduction of the contact resistance[45] and diffusion of mobile charges. Devices without mask can lead to a large overestimation of R and estimation of R becomes strongly V_{gate} dependent as shown in Figure 4b except at around $V_{gate} = -14$ V. At around $V_{gate} = -14$ V, R is nearly independent of intensity, possibly because the potential is near to the flat-band voltage. R not only depends on V_{gate} but also strongly depends on the intensity of illumination. The lower the intensity, the higher is R, as depicted in Figure 4b. This is one of the advantages of using OFETs as photodetector, as their sensitivity increases at lower illumination intensities while being tunable by V_{gate}. The reason for lower R at higher intensity is not clear yet. However, Hamilton et al.[27] gave a plausible reason based on the saturation of photocurrent, I_{ph} ($=I_{drain} - I_{dark}$). Saturation in I_{ph} can be caused by several factors including the efficiency of charge transport through the channel region at higher intensity and exciton–exciton annihilation. Previous reports have shown different trends of R with increasing intensity depending on the wavelength of illumination.[22,23] The largest measured R of the bilayer devices, 11 A W^{-1} at 532 nm is among the highest reported values of all organic devices and comparable to the values reported in two recent reports by Narayan and Kumar on single layer poly [3-hexylthiophene] (P3HT) OFETs[11] and Noh et al. on single layer 2,5-dibromothieno[3,2-b]thiophene (BPTT).[22]

R is not only V_{gate} dependent but also depends on the side from which the device is illuminated. This can be attributed to the location of free carriers due to absorbed photons in the semiconducting film with respect to its conducting channel in the OFET. Since we used optically transparent BCB as a dielectric and transparent ITO as a gate electrode, it allows illumination from both sides of the OFETs. When illuminating from the Al side, the bulk film absorbs most of the light intensity and hence a large bulk current is observed in the depletion regime and a small light response at higher accumulation V_{gate} as shown in Figure 4a. The effect of the bulk current was further investigated by measuring the transistor output characteristics at floating V_{gate} as shown in Figure 4c. Devices with mask show a linear regime at low drain voltage, V_{drain}, and saturated I_{drain} at higher V_{drain} upon illumination as if there was an external applied positive V_{gate}. Devices without mask show a mixed response of linear and saturation I_{drain} showing an almost constant differential resistance with increasing V_{drain}. To avoid the effects originating in this bulk current, all our further experiments are carried out on devices with mask which allows us to directly compare I_{ph} on the side at which the illumination occurs. I_{ph} is compared for both sides of illumination with 532 and 780 nm light with the same ϕ as shown in Figure 5a and b, respectively. As can be seen in Figure 5b, the illumination with 780 nm only gives rise to an I_{ph} on the bilayer system. In the device without ZnPc, no photoinduced currents can be measured. There exists no significant difference on the side from which the illumination occurs in bilayer devices for 780 nm light. This results further supports i) PICT,[43,44] and ii) effective charge transport in the vicinity of the conductive channel when charges are created at the interface.[7,10] However, a large number of photoinduced charge carriers at the interface cannot be depleted and I_{ph} remains high even with an applied depletion V_{gate}, as reflected in Figure 5b.

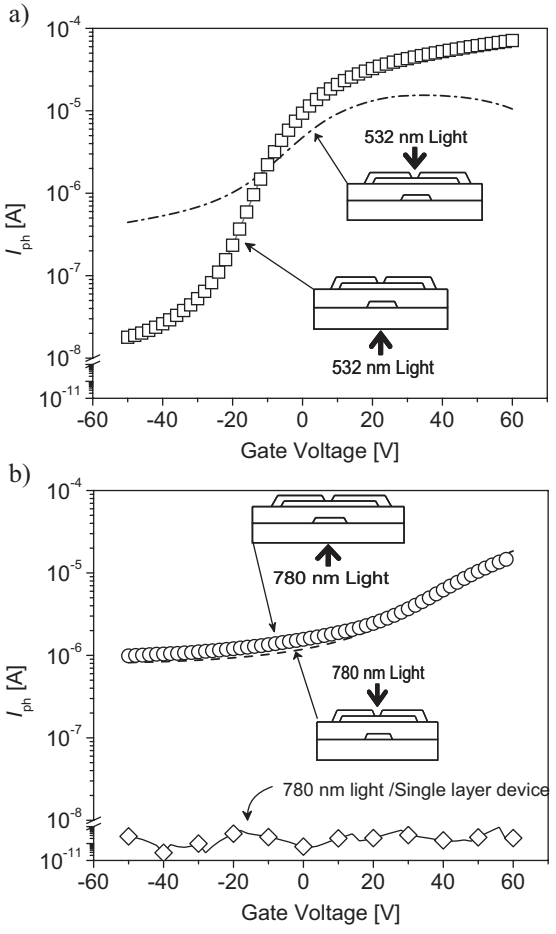

Figure 5. Comparison of I_{ph} versus V_{gate} in the saturation regime ($V_D = 20$ V) for the masked devices for single layer and bilayer devices upon illumination of a) 532 nm and b) 780 nm both with photon flux of 1.1×10^{16} photons cm^{-2} s^{-1}. There exists no significant difference on the side from which the illumination occurs for 780 nm on bilayer devices.

2.3. Bilayer OFETs in Linear Regime and Upon Illumination

It is now clear that there exists PICT between ZnPc and fullerene giving rise to photoinduced carriers. From now on, we operate the bilayer OFET in the linear regime of V_D (<6 V). By operating the bilayer OFET in the linear regime where the applied gate field is much larger than the in-plane drift field, this results in an approximately uniform charge carrier density in the active channel. Further, to avoid the effect of the absorption in both layers, a wavelength of 780 nm is chosen, where the C_{60} layer is transparent and the light is only absorbed in the ZnPc islands. The subsequent PICT will then generate electrons in the C_{60} layer in the vicinity of the semiconductor/dielectric interface. Thus a direct comparison between the channel formation via an applied electric field or by PICT becomes possible. The transfer characteristics in the linear regime (at a low $V_{drain} = 6$ V) are shown in Figure 6. The applied gate field in this regime is much larger than the in-plane drift field, which results in an approximately uniform density of charge carriers in the active channel. The linear μ_{FE} calculated using Equation 1, without

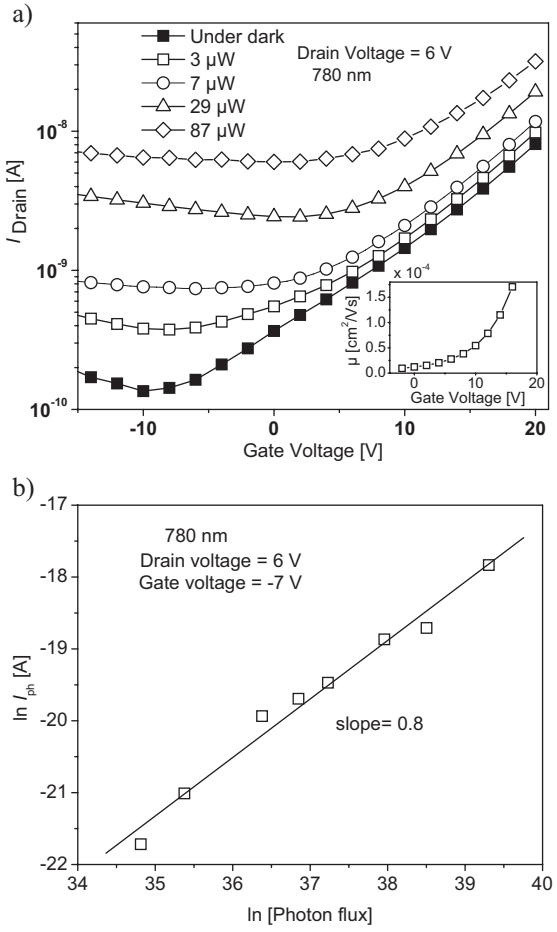

Figure 6. a) Linear transfer characteristics at low drain voltage of 6 V under dark and upon illumination with mask at with various intensities for the bilayer devices; inset shows the linear mobility as a function of V_{gate}. b) Plot of $\ln I_{ph}$ versus $\ln\phi$ (squares) with applied V_{gate} of −7 V and linear fit (solid line) to the data.

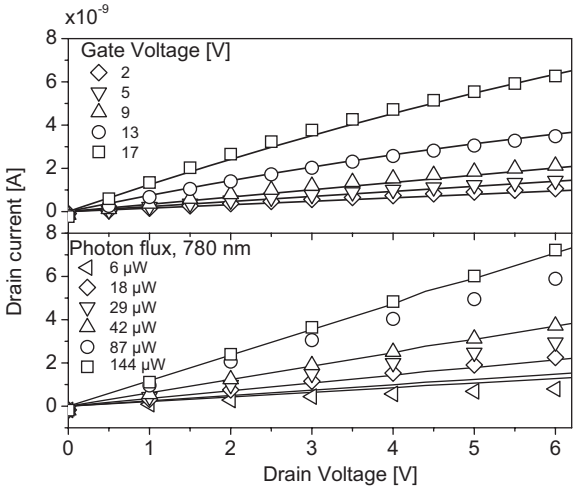

Figure 7. Upper panel: Linear output characteristics under dark (symbols) and the computed (solid line) *I–V* characteristics for the bilayer devices with μ data taken from Figure 6a with $C_{ins} = 5.7 \times 10^{-9}$ nF cm^{-2} and $V_{th} = -7$ V using Equations 1 and 2. Lower panel: Plot of I_{drain} versus V_{drain} (symbols) with applied V_{gate} ($=V_{th}$) of −7 V for different intensities of 780 nm light and the computed (solid lines) using Equations 1 and 2 assuming $C_{ins} = 5.7 \times 10^{-9}$ nF cm^{-2} with V_{gate} of 2, 5, 9, 13, 17 V and μ values taken from Figure 6a.

taking the contact resistance into account is evaluated from the $I_{drain} - V_{gate}$ (V_{th} of −7 V) characteristics as shown in the inset of Figure 6a. Upon illumination, I_{drain} increases gradually with increasing light intensity. The minimum drain current measured for the applied V_{drain} (6 V) goes to higher values upon increasing the illumination intensity which is equivalent to the additional capacitance of an applied gate field.

The I_{ph} changes linearly with ϕ as shown in the plot of $\ln(I_{ph})$ versus $\ln(\phi)$ in Figure 6b. From this measurement, it can be deduced that the number of photogenerated charge carriers also increases linearly at low ϕ. To verify if the external applied gate field can be completely replaced by PICT and to visualize the charge accumulation in the conducting channel of the OFET, we performed the following measurements: i) output characteristics in the linear regime of the OFET with applied gate field and ii) output characteristics in the linear regime of the OFET with fixed external applied V_{gate} of −7 V and illuminating with varying illuminating intensity, thus repeating the measurement (i) using a photoinduced gate effect. A fixed V_{gate} of −7 V is applied because it gives the lowest I_{dark}. The output curves with different applied gate fields are plotted in the upper panel of Figure 7. The output curves with varying illumination intensities are plotted in the lower panel in Figure 7. The lines are theoretical fits using Equation 1 and 2 and assuming linear μ_{FE} values obtained from the measurement as shown in Figure 6a. Similarly, the values for I_{drain} in the case of photogating are also fitted using Equation 1 and 2 assuming a virtually applied gate field. These measurements indicate that one can produce photoinduced free carriers at the interface of the active semiconducting layer and form a conducting channel without an externally applied gate field.

It is also well known from the literature that charges are accumulated at the semiconductor very close to the interface of the gate dielectric upon applied V_{gate}. This allows us to calculate the charge carrier density, Q, either by using $Q = J/\mu_{FE}E$, where J is the drain current density and E is the electric field; or by using $Q = C_{ins} \times V_{gate}$ and also the V_{gate} equivalent charges due to the photoinduced phenomena at the conducting channel. An analysis of the V_{gate} equivalent photoinduced charge carrier density at the interface which formed the conducting channel is shown in the upper panel of Figure 8. From the measurement of ϕ and resulting V_{gate} equivalent photoinduced charge carrier density, EQE is estimated to be 10^{-5}–10^{-4} as shown in the lower panel of Figure 8. The estimated EQE is only true for the excitation wavelength of 780 nm and will be dependent on the excitation wavelength. Finally, IQE can be estimated with the knowledge of the amount of photons absorbed in the 5 nm of ZnPc layer. Assuming an absorption coefficient of 1.5×10^4 cm^{-1}, the highest IQE estimated is in the order of 2.5%. This means that 1 in every 40 photons absorbed in the ZnPc will give rise to a charge carrier taking part in the conducting channel formation upon illumination with small intensity 780 nm light. IQE saturates toward values of about 0.1% at high light intensities.

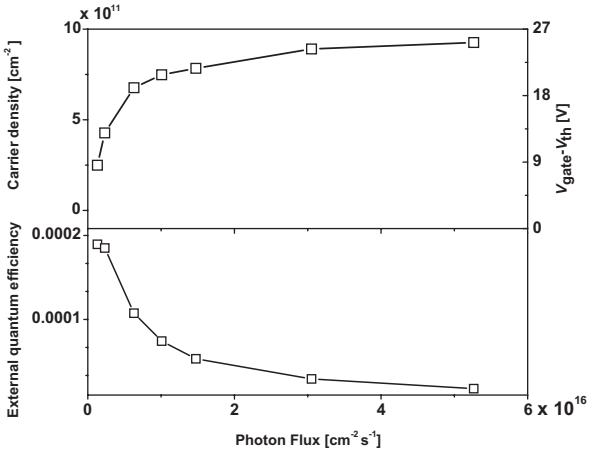

Figure 8. Upper panel: Plot of equivalent carrier density extracted from Figure 7a and b with corresponding C_{ins} and V_{gate} versus ϕ of 780-nm light. Note that $V_{gate} - V_{th}$ is plotted in the right Y-axis. Lower panel: Plot of EQE versus ϕ.

Very low level light will give even higher IQE values, but the absolute current values are very low, making an accurate estimation difficult.

3. Conclusions

In summary, we have exploited the phenomena of PICT between ZnPc and C_{60} layers to simulate the charge carrier accumulation in OFETs. An applied V_{gate} to form a conducting channel in an OFET can be replaced by illumination at a wavelength where only the ZnPc is absorbing. The method uses a completed OFET device and operation of the OFET in the linear regime, where the applied gate field is much larger than the in-plane drift field, which results in an approximately uniform charge carrier density in the active channel. Thus, a direct comparison between the channel formation via an applied electric field or by photo-generated charge transfer becomes possible. This experiment can be performed to evaluate the efficiency of photoinduced charge generation between two organic semiconductor materials. Further optimization of this experiment can lead to the determination of diffusion lengths of charge carriers. For the present experiment with minimized artefacts, a large R of 10^{-3}–10^{1} A W^{-1} depending on the intensity of illumination and on applied V_{gate} could be obtained. This makes these devices good candidates for amplified organic photodetectors.

4. Experimental

Device Fabrication: OFETs were fabricated using transparent ITO-coated glasses as gate electrode/substrate. The ITO was etched leaving an area of 0.5 mm × 15 mm as a gate electrode. ITO glasses were cleaned using acetone, 2-propanol, Helmanex glass cleaning solution, and finally with deionized H_2O in an ultrasonic bath. Divinyltetramethyldisiloxane-bis(benzocyclobutene) (BCB) [38,41], purchased from Dow Chemicals, was spin coated on top of the ITO substrate as a transparent gate dielectric. The area of the BCB gate dielectric was optimized by removing the thin film with the mesitylene solvent and subsequently cured at 250 °C for 2 h in vacuum oven. ZnPc was obtained from Sigma–Aldrich Co. and further purified by train sublimation. C_{60} purified by sublimation to >99.9% was used as received from MER Corp. Following the BCB curing, a 5-nm layer of ZnPc followed by a 300-nm-thick film of C_{60} was grown by organic vapour phase deposition at T_s of 25 °C. The organic thin films were grown at a rate of 0.2–0.3 Å s^{-1} in a base vacuum of 10^{-6} mbar using a Leybold Univex 350 with a source to substrate height of about 0.5 m. The reference devices with only C_{60} as a semiconductor are described as single layer and devices with active C_{60} layer grown on top of ZnPc islands are described as bilayer. Device fabrication was completed by the evaporation of top-contact electrodes consisting of LiF/Al (0.6 and 60 nm, respectively) under high vacuum (~10^{-6} torr) through a shadow mask. The channel length (L) and width (W) of the transistor was 30 μm and 1.5 mm, respectively. The average thickness of the dielectric was about 1–1.5 μm. Measured dielectric capacitance in inert condition with the thickness of the dielectric layer consistently gave the values of the dielectric constant, ε of 2.6; capacitance, C_i of 1.2 nF cm^{-2}.

Device Characterization: Device transportation from the evaporation chamber to the glove box for metal evaporation was carried out under ambient condition. All electrical and optical characterization was carried out in an Oxford Instrument DNV Optistat with a base pressure of 10^{-6}mbar. An Agilent E5273A with two source-measure unit instruments was employed for the steady state current-voltage measurements. Keithley 2400 and 236 source-measure unit instruments were also employed to reconfirm all the electrical measurements. To avoid any device stress related threshold voltage shift, consecutive measurements are performed with long enough waiting. All measurements were performed with a scan rate of 2 V s^{-1} unless otherwise stated. For illuminating the devices, we used 150-μm-thick stainless steel masks to cover everything except the channel area of the device. For 532-nm monochromatic light illumination, a Coherent Verdi laser was employed and for 780-nm illumination, a diode laser was used.

Surface Characterization of Thin Films: The thin film morphology of 5-nm ZnPc film was also studied by using SEM. The SEM images were acquired using a Zeiss 1540XB microscope.

UV–Vis Spectra: Spectra were acquired using Cary 3G UV–Vis Spectrophotometer on the reference thin films prepared at the same condition as described for OFETs.

Acknowledgements

We gratefully acknowledge partial financial support from Austrian National Science Foundation (FWF). We also wish to cordially thank DI Günter Hesser from Institute of Semiconductor and Solid State Physics, Johannes Kepler University for providing the surface electron microscope (SEM) images.

Received: September 26, 2008
Revised: October 30, 2008
Published online: January 29, 2009

[1] For a recent review on conjugated polymer based solar cells, see: S. Guenes, H. Neugebauer, N. S. Sariciftci, *Chem. Rev.* **2007**, *107*, 1324.
[2] T. Morimume, H. Kajii, Y. Ohmori, *IEEE Photonics Technol. Lett.* **2006**, *18*, 2662.
[3] G. Horowitz, in *Semiconducting polymers, chemistry, Physics and Engineers*, (Eds: G. Hadziioannou, G. Malliaras), Wiley-VCH, Weinheim, Germany **2007**, Ch. 12.
[4] T. Ng. Ng, W. S. Wong, M. L. Chabilnyc, S. Sambandan, R. A. Street, *Appl. Phys. Lett.* **2008**, *92*, 213303.
[5] a) D. Moses, H. Okumoto, H. Lee, A. J. Heeger, T. Ohnishi, T. Noguchi, *Phys. Rev. B* **1996**, *54*, 4748. b) C. H. Lee, G. Yu, A.J. Heeger, *Phys. Rev. B* **1993**, *47*, 15543.

[6] L. A. A. Petterson, L. S. Roman, O. Inganas, *J. Appl. Phys.* **2001**, *89*, 5564.
[7] F. Dinelli, M. Murgia, P. Levy, M. Cavallini, F. Biscarini, D. M. De Leeuw, *Phys. Rev. Lett.* **2004**, *92*, 116802.
[8] G. Horowitz, *J. Mater. Res.* **2004**, *19*, 1949.
[9] R. Ruiz, A. Papadimitratos, A. C. Mayer, G. G. Malliaras, *Adv. Mater.* **2005**, *17*, 1795.
[10] J. Lee, K. Kim, J. H. Kim, S. Im, D.-Y. Jung, *Appl. Phys. Lett.* **2003**, *82*, 4169.
[11] K. S. Narayan, N. Kumar, *Appl. Phys. Lett.* **2001**, *79*, 1891.
[12] S. Man Mok, F. Yan, H. L. W. Chan, *Appl. Phys. Lett.* **2008**, *93*, 023310.
[13] D. Knipp, D. K. Murti, B. Krusor, R. Apte, L. Jiang, J. P. Lu, B. S. Ong, R. A. Street, *Mater. Res. Soc. Symp. Proc.* **2001**, *665*, C5.44.1.
[14] J.-M. Choi, J. Lee, D. K. Hwang, J. H. Kim, S. Im, E. Kim, *Appl. Phys. Lett.* **2006**, *88*, 043508.
[15] M. Breban, D. B. Romero, S. Mezhenny, V. W. Ballarotto, E. D. Williams, *Appl. Phys. Lett.* **2005**, *87*, 203503.
[16] M. Debucquoy, S. Verlaak, S. Steudel, K. Myny, J. Genoe, P. Heremans, *Appl. Phys. Lett.* **2007**, *91*, 103508.
[17] Y. Hu, G. Dong, C. Liu, L. Wang, Y. Qiu, *Appl. Phys. Lett.* **2006**, *89*, 072108.
[18] S. M. Cho, S. H. Han, J. H. Kim, J. Jang, M. H. Oh, *Appl. Phys. Lett.* **2006**, *88*, 071106.
[19] J.-M. Choi, K. Lee, D. K. Hwang, J. H. Kim, S. Im, J. H. Park, E. Kim, *J. Appl. Phys.* **2006**, *100*, 116102.
[20] J.-M. Choi, K. Lee, D. K. Hwang, J. H. Kim, S. Im, E. Kim, *Appl. Phys. Lett.* **2006**, *88*, 043508.
[21] N. Mathews, D. Fichou, E. Menard, V. Podzorov, S. G. Mhaisalkar, *Appl. Phys. Lett.* **2007**, *91*, 212108.
[22] Y.-Y. Noh, D.-Y. Kim, Y. Yoshida, K. Yase, B. Jung, E. Lim, H.-K. Shim, *Appl. Phys. Lett.* **2005**, *86*, 043501.
[23] Y.-Y. Noh, D.-Y. Kim, K. Yase, *J. Appl. Phys.* **2005**, *98*, 074505.
[24] S. Dutta, K. S. Narayan, *Appl. Phys. Lett.* **2005**, *87*, 193505.
[25] S. Dutta, K. S. Narayan, *Synth. Met.* **2004**, *146*, 321.
[26] M. C. Hamilton, J. Kanicki, *IEEE J. of Sel. Top. Quantum Electron.* **2004**, *10*, 1077.
[27] M. C. Hamilton, S. Martin, J. Kanicki, *IEEE Trans. Electron Devices* **2004**, *51*, 876.
[28] T. P. I. Saragi, R. Pudzich, T. Fuhrmann, J. Salbeck, *Appl. Phys. Lett.* **2004**, *84*, 2334.
[29] T. P. I. Saragi, T. Spehr, A. Siebert, T. Fuhrmann-Lieker, J. Salbeck, *Chem. Rev.* **2007**, *107*, 1011.
[30] Y. Xu, P. R. Berger, J. N. Wilson, U. H. F. Bunz, *Appl. Phys. Lett.* **2004**, *85*, 4219.
[31] M. Yonezawa, H. Kimura, Y. Yamazaki, J. Koyama, Y. Watanabe, Method of Manufacturing a Semiconductor Devices. *US Patent #* 7351605, **2008**.
[32] K. S. Narayan, Photoresponsive Organic Field-Effect Transistors. *US Patent #* 6992322, **2006**.
[33] Th. B. Singh, F. Meghdadi, S. Guenes, N. Marjanovic, G. Horowitz, P. Lang, S. Bauer, N. S. Sariciftci, *Adv. Mater.* **2005**, *17*, 2315.
[34] L. L. Chua, J. Zaumseil, J. Chang, E. C. W. Ou, P. K. H. Ho, H. Sirringhaus, R. H. Friend, *Nature* **2005**, *434*, 194.
[35] S. Cho, J. Yuen, J. Y. Kim, K. Lee, A. J. Heeger, *Appl. Phys. Lett.* **2007**, *90*, 063511.
[36] N. Marjanovic, Th. B. Singh, G. Dennler, S. Guenes, H. Neugebauer, N. S. Sariciftci, R. Schwödiauer, S. Bauer, *Org. Eletron.* **2006**, *7*, 188.
[37] T. D. Anthopoulos, *Appl. Phys. Lett.* **2007**, *91*, 113513.
[38] Th. B. Singh, N. Marjanović, G. J. Matt, S. Gunes, N. S. Sariciftci, A. Montaigne Ramil, A. Andreev, H. Sitter, R. Schwödiauer, S. Bauer, *Org. Electron.* **2005**, *6*, 105.
[39] J. Locklin, K. Shinbo, K. Onishi, F. Kaneko, Z. Bao, R. C. Advincula, *Chem. Mater.* **2003**, *15*, 1404.
[40] L. L. Chua, P. K. H. Ho, H. Sirringhaus, R. H. Friend, *Appl. Phys. Lett.* **2004**, *84*, 3400.
[41] Th. B. Singh, N. Marjanović, P. Stadler, M. Auinger, G. J. Matt, S. Gunes, N. S. Sariciftci, R. Schwödiauer, S Bauer,, *J. Appl. Phys.* **2005**, *97*, 083714.
[42] Y.-L. Lee, W.-C. Tsai, J.-T. Maa, *Appl. Surf. Sci.* **2001**, *173*, 352.
[43] M. E. El-Khouly, O. Ito, P. M. Smith, F. D'Souza, *J. Photochem. Photobiol. C* **2004**, *5*, 79. DOI: 10.1016/j.jphotochemrev.2004.01.003.
[44] R. Koeppe, N. S. Sariciftci, *J. Photochem. Photobiol. Sci.* **2006**, *5*, 1122.
[45] M. Rao, K. S. Narayan, *Appl. Phys. Lett.* **2008**, *92*, 223308.